# Optimal Operation of Active Distribution Systems with Voltage Control and Closed-Loop Topology

Juan M. Home-Ortiz, Leonardo H. Macedo, José R. S. Mantovani, Rubén Romero
*Department of Electrical Engineering, São Paulo State University–UNESP*
Ilha Solteira, Brazil
juan.home@unesp.br, leohfmp@ieee.org, mant@dee.feis.unesp.br, ruben.romero@unesp.br

Renzo Vargas
*UFABC*
Santo André, Brazil
renzo@ieee.org

João P. S. Catalão
*FEUP and INESC TEC*
Porto, Portugal
catalao@fe.up.pt

2021 IEEE Madrid PowerTech | 978-1-6654-3597-0/21/$31.00 ©2021 IEEE | DOI: 10.1109/PowerTech46648.2021.9495076

***Abstract*—This paper presents a new stochastic mixed-integer second-order cone programming model to solve the problem of optimal operation of distribution systems considering network reconfiguration, voltage control devices, dispatchable and nondispatchable distributed generators (DGs), and the possibility of closed-loop topology operation. The decision variables are the active and reactive power generation of DGs, the tap position of substations' (SS) on-load tap changers and voltage regulators, the number of switchable capacitor banks in operation, and the operational statuses of sectionalizing and tie switches. The proposed formulation considers the minimization of (i) the cost of the energy purchased from the distribution SSs and dispatchable DGs, (ii) greenhouse gas emissions, (iii) technical energy losses, and (iv) the number of basic loops formed in the network. Tests are carried out using the 33-node system and the results demonstrate the effectiveness of the proposed formulation. The benefits provided by the presented approach include reduced operational costs and greenhouse gas emissions mitigation.**

***Index Terms*—*Closed-loop topology, distributed generation, distribution systems reconfiguration, mixed-integer second-order cone programming, voltage-dependent models.***

## I. Introduction

The problem of optimal operation of active distribution systems addresses the efficient and economical operation of power distribution systems in normal state. Thus, it determines the optimal settings for a group of decision variables, including the tap positions of substations' (SS) on-load tap changers (OLTCs) and voltage regulators (VRs), the number of switchable capacitor banks (CBs) in operation, active and reactive power injections from dispatchable distributed generators (DGs), and the operation state of sectionalizing and tie switches. In this paper, the objective is to simultaneously minimize (i) the cost of the energy purchased from the distribution SSs and dispatchable DGs, (ii) greenhouse gas emissions, (iii) the costs related to technical energy losses, and (iv) the number of basic loops [1] formed in the network.

The works available in the literature do not consider the simultaneous control of all the devices previously cited. Also, these works disregard the possibility of closed-loop topologies for the network in normal state operation, therefore, only radial configurations are allowed. Many works use heuristics and metaheuristics as solution techniques to solve the problem [2]–[9]. In [2], an evolutionary algorithm is proposed for the optimal operation problem of distribution systems considering network reconfiguration and the operation of CBs and SSs' OLTCs. In [3], the authors recognize the importance of a centralized adjustment of voltage control devices in the presence of renewable sources for avoiding operational problems due to reverse power flows. However, as the operation of these devices is still autonomous, based on local signals, the authors propose a coordinated approach for VRs, OLTCs, and photovoltaic (PV) generation units for minimizing the number of tap operations of VRs. In [4], two algorithms are presented for the optimal operation of distribution systems considering CBs, VRs, and DGs. The first algorithm is a Chu-Beasley's genetic algorithm. The second procedure is a simplified algorithm capable of obtaining good quality solutions with lower computational effort. Reference [5] proposes an NSGA-II-based multi-objective approach for peak-load relief and energy efficiency in distribution systems. For these purposes, the operation of OLTCs, VRs, and CBs are considered. In [6], a sunflower optimization-based algorithm is proposed for the optimal power flow in power systems including DGs. The main objective of the problem is established as optimizing the generating units' fuel costs. In [7], a modified binary gray wolf optimization algorithm is proposed for the reduction of energy consumption and energy losses in distribution systems. In the proposed approach, the operation of OLTCs, VRs, CBs, as well as system reconfiguration and PV smart inverters are considered for the energy savings problem. Reference [8] proposes a chaos disturbed beetle antennae search algorithm for the multi-objective system reconfiguration considering variations in load and DGs in distributions systems. As such, the problem is formulated considering three conflicting objectives: to minimize active power losses, to improve the load balancing index, and to minimize the sum of maximum nodal voltages deviation index. In [9], the distribution system performance enhancement is addressed by the simultaneous operation of CBs, DGs, and distribution system reconfiguration. To tackle this objective, a tunicate swarm algorithm is proposed.

Exact methods and mathematical optimization models are also used to tackle this problem [10]–[17]. In [10], a Benders decomposition technique is proposed for minimizing power losses in distribution systems considering network reconfiguration and the presence of DGs. The formulation of the problem is embedded in two stages. The first stage is the master problem formulated as a mixed-integer nonlinear programming (MINLP) problem. The second stage is the slave problem, formulated as a nonlinear programming (NLP) problem. In [11], a mixed-integer linear programming (MILP) formulation is proposed for minimizing energy losses in a distribution system considering PV generation and the possibility of network reconfiguration. Reference [12] proposes an MILP model considering the operation of VRs, CBs, and DGs for the optimal operation of distribution systems. In [13], an MINLP problem is reformulated into an NLP formulation for solving the optimal operation problem. The proposed model aims to minimize the energy consumption from the distribu-

This work was supported by the Coordination for the Improvement of Higher Education Personnel (CAPES) – Finance Code 001, the Brazilian National Council for Scientific and Technological Development (CNPq), grants 305852/2017-5 and 305318/2016-0, the São Paulo Research Foundation (FAPESP), under grants 2015/21972-6, 2018/20355-1, 2019/19632-3, 2019/01841-5, and 2019/23755-3, and by ENEL under the grant: PEE-00390-1062/2017 - P&D-00390-1083-2020_UFABC, ANEEL 001-2016.

tion SS, as well as minimizing the number of switching operations of OLTCs and CBs. Reference [14] proposes a coordinated approach for the optimal operation of distribution systems. This coordinated approach considers network reconfiguration and the operation of VRs and distributed energy resources. In [15], the authors present an optimal power flow-based approach for the conservation voltage reduction problem. As such, a centralized scheme is proposed for controlling OLTCs and CBs, considering high PV penetration levels. The problem is formulated as an NLP problem by relaxing integer variables for scalability purposes. In [16], a distributed optimization method is proposed for minimizing the active power losses and PV generation losses by adjusting voltage control devices, such as reactive power compensators, step VRs, and PV inverters. Reference [17] proposes a two-stage approach for the optimal voltage regulation problem. The proposed approach uses the available reactive power of DGs and the OLTCs in distribution SSs. This method follows a rule-based method to create a Pareto front considering two conflicting objectives: system energy losses and tap changes frequency.

Some works highlight the benefits that closed-loop topologies could bring to the operation of distribution systems. In [18], the authors propose a feasibility study for upgrading primary feeders from radial configurations to closed-loop arrangements. In [19] an MINLP model is presented for minimizing losses in a distribution system. An important conclusion of this work is that not necessarily an all-closed-switches topology is the best arrangement for reducing energy losses. A radial configuration is the topology with the largest value of energy losses, and as tie switches are sequentially closed forming loops, the energy losses of the system are reduced. However, the optimal solution does not necessarily have all branches connected. Thus, the number of basic loops for optimal energy loss reduction must be calculated. In this work, we determine the best closed-loop topology in steady-state operation to optimize the operation of active distribution systems.

The main contribution of this paper is a new stochastic mixed-integer second-order cone programming (MISOCP) model for the problem of optimal operation of active distribution systems that considers a voltage-dependent load model, the operation of voltage control devices, such as CBs, OLTCs, and VRs, the optimal operation of dispatchable DGs, PV units, and the reconfiguration of the network with closed-loop operation and control in the number of basic loops formed. The MISOCP formulation guarantees convergence to the optimal solution of the problem by using existing classical optimization techniques.

## II. Problem Formulation

### A. Objective Function

The formulation optimizes the operational costs of the SSs and DGs while minimizing the number of basic loops formed. Equation (1) presents the objective function of the problem.

$$\text{minimize}\, \psi = C^{SS} + C^{DG} + C^{LS} + C^{LP} \tag{1}$$

in which:

$$C^{SS} = \sum_{i\in\Omega_{SS}} \sum_{t\in\Omega_T} \sum_{s\in\Omega_S} \pi_{t,s}\Delta_t(\varsigma^{SS}_{t,s} P^{SS}_{i,t,s} + \varsigma^{EM}\epsilon^{SS} P^{SS}_{i,t,s}) \tag{2}$$

$$C^{DG} = \sum_{i\in\Omega_{DG}} \sum_{t\in\Omega_T} \Delta_t(\varsigma^{DG}_{i,t} P^{DG}_{i,t} + \varsigma^{EM}\epsilon^{DG}_{i} P^{DG}_{i,t}) \tag{3}$$

$$C^{LS} = \sum_{ij\in\Omega_B} \sum_{t\in\Omega_T} \sum_{s\in\Omega_S} \varsigma^{LS}\pi_{t,s}\Delta_t R_{ij} I^{SQ}_{ij,t,s} \tag{4}$$

$$C^{LP} = \varsigma^{LP}\left[\sum_{ij\in\Omega_B} w^{SW}_{ij} + |\Omega_{VR}| - (|\Omega_N| - |\Omega_{SS}|)\right] \tag{5}$$

In the objective function $\psi$, shown in (1), $C^{SS}$ is the operational cost of the SSs, $C^{DG}$ is the operational cost of the DGs, $C^{LS}$ is the cost of losses, and $C^{LP}$ is the cost of loop formation. In these equations, $\Omega_N$ is the set of nodes, indexed by $i$, $\Omega_{SS}$ is the set of SS nodes, $\Omega_{DG}$ is the set of nodes with DGs, $\Omega_B$ is the set of branches, indexed by $ij$, $\Omega_{VR}$ is the set of OLTCs and VRs, $\Omega_T$ is the set of time intervals, indexed by $t$, and $\Omega_S$ is the set of scenarios, indexed by $s$. The parameter $\Delta_t$ is the duration of a time interval, $\pi_{t,s}$ is the probability of realization of a scenario, $\varsigma^{SS}_{t,s}$ is the energy price at the SSs, $\varsigma^{DG}_{i,t}$ is the energy price of the DGs, $\varsigma^{LS}$ is the price of losses, $\varsigma^{LP}$ is a price for loop formation, $\varsigma^{EM}$ is the price of emissions, $\epsilon^{SS}$ is the rate of emissions by the SSs, $\epsilon^{DG}_i$ is the rate of emissions of the DGs, and $R_{ij}$ is the resistance of a branch. The variable $P^{SS}_{i,t,s}$ is the active power injected by a SS, $P^{DG}_{i,t}$ is the active power injected by a DG, $I^{SQ}_{ij,t,}$ is the square value of the current on a branch, and $w^{SW}_{ij}$ is the binary variable that indicates the status of the switch on a branch, i.e., if $w^{SW}_{ij} = 0$ the switch is open and if $w^{SW}_{ij} = 1$ the switch is closed.

Equation (2) is the operational cost of the SSs, accounting for both the cost of the energy and emissions cost, (3) is the operational cost of the DGs, including both the generation cost and the emissions cost, (4) is the cost of losses, and (5) is the cost of loop formation (the formation of loops is controlled by (37)–(40)).

### B. Power Flow Constraints

The ac operation of the system is represented by the power flow equations (6)–(13).

$$\sum_{ji\in\Omega_B} P_{ji,t,s} - \sum_{ij\in\Omega_B}(P_{ij,t,s} + R_{ij} I^{SQ}_{ij,t,s}) + \sum_{ji\in\Omega_{VR}} P^{VR}_{ji,t,s} - \sum_{ij\in\Omega_{VR}} P^{VR}_{ij,t,} + P^{SS}_{i,t,s} + P^{DG}_{i,t} + P^{PV}_{i,t,s} = P^{D}_{i,t,s}\left[\gamma^{Z}_{i,t,s}\frac{V^{SQ}_{i,t,s}}{(V^N)^2} + \gamma^{I}_{i,t,s}\frac{V_{i,t,s}}{V^N} + \gamma^{P}_{i,t,s}\right] \tag{6}$$

$$\sum_{ji\in\Omega_B} Q_{ji,t,s} - \sum_{ij\in\Omega_B}(Q_{ij,t,s} + X_{ij} I^{SQ}_{ij,t,s}) + \sum_{ji\in\Omega_{VR}} Q^{VR}_{ji,t,s} - \sum_{ij\in\Omega_{VR}} Q^{VR}_{ij,t,} + Q^{SS}_{i,t,s} + Q^{DG}_{i,t} + Q^{PV}_{i,t,s} + \hat{Q}^{CB}_{i,t,s} = Q^{D}_{i,t,s}\left[\mu^{Z}_{i,t,s}\frac{V^{SQ}_{i,t,s}}{(V^N)^2} + \mu^{I}_{i,t,s}\frac{V_{i,t,s}}{V^N} + \mu^{P}_{i,t,s}\right] \tag{7}$$

$$V_{i,t,s} = \sqrt{\frac{\overline{V}+\underline{V}}{2}} + \frac{1}{2\sqrt{\frac{\overline{V}+\underline{V}}{2}}}\left(V^{SQ}_{i,t,s} - \frac{\overline{V}+\underline{V}}{2}\right) \tag{8}$$

$$\forall i \in \Omega_N, t \in \Omega_T, s \in \Omega_S$$

$$V^{SQ}_{i,t,s} - V^{SQ}_{j,t,s} + \zeta_{ij,t,s} = 2(R_{ij}P_{ij,t,s} + X_{ij}Q_{ij,t,s}) + Z^2_{ij} I^{SQ}_{ij,t,s} \tag{9}$$

$$\hat{v}_{i,t,s}\hat{v}_{j,t,s}(\theta_{i,t,s} - \theta_{j,t,s} + \xi_{ij,t,s}) = X_{ij}P_{ij,t,s} - R_{ij}Q_{ij,t,s} \tag{10}$$

$$V^{SQ}_{j,t,s} I^{SQ}_{ij,t,s} \geq P^2_{ij,t,s} + Q^2_{ij,t,s} \tag{11}$$

$$|\zeta_{ij,t,s}| \leq M^V(1 - w^{SW}_{ij}) \tag{12}$$

$$|\xi_{ij,t,s}| \leq M^\Theta(1 - w^{SW}_{ij}) \tag{13}$$

$$\forall ij \in \Omega_B, t \in \Omega_T, s \in \Omega_S$$

In (6)–(13), the parameters $P^D_{i,t,s}$ and $Q^D_{i,t,s}$ are the active and reactive power demands at nominal voltage, $\gamma^Z_{i,t,s}$, $\gamma^I_{i,t,s}$, and $\gamma^P_{i,t,s}$ are the active load components of constant impedance, current, and power, $\mu^Z_{i,t,s}$, $\mu^I_{i,t,s}$, and $\mu^P_{i,t,s}$ are the reactive

load components of constant impedance, current, and power of the voltage-dependent ZIP load model [20], $X_{ij}$ is the reactance of a branch, $Z_{ij}$ is the magnitude of the impedance of a branch, $V^N$ is the nominal voltage of the system, $\underline{V}$ and $\overline{V}$ are the minimum and maximum voltage magnitude limits, $\hat{v}_{i,t,s}$ is an estimate for the voltage magnitude, and $M^V$ and $M^\Theta$ are parameters used in the big-M formulation. The variables $P_{ij,t,s}$ and $Q_{ij,t,}$ are the active and reactive power flows on the branches, $P^{VR}_{ij,t,}$ and $Q^{VR}_{ij,t,s}$ are the active and reactive power flows on OLTCs and VRs, $Q^{SS}_{i,t,s}$ is the reactive power injected by a SS, $Q^{DG}_{i,t}$ is the reactive power injected by a DG, $P^{PV}_{i,t,s}$ and $Q^{PV}_{i,t,s}$ are the active and reactive power injected by a PV unit, $V_{i,t,s}$ and $V^{SQ}_{i,t,s}$ are the voltage magnitude and its square value at a node, $\theta_{i,t,s}$ is the voltage phase angle at a node, $\hat{Q}^{CB}_{i,t,s}$ is the total reactive power injected by a CB, and $\zeta_{ij,t,}$ and $\xi_{ij,t,}$ are slack variables.

Constraints (6) and (7) are the active and reactive power balance constraints, respectively, representing the application of Kirchhoff's current law to the system, (8) calculates the voltage magnitude at a node from the value of the squared voltage magnitude, and (9)–(13) represent the systematic application of Kirchhoff's voltage law to the system, in which (12) and (13) are used to calculate the slack variables $\zeta_{ij,t,s}$ and $\xi_{ij,t,}$ according with the statuses of the switches.

### C. Physical and Operational Limits of the System

Constraints (14)–(18) are the physical and operational limits of the system.

$$0 \le I^{SQ}_{ij,t,s} \le \overline{I}^2_{ij} w^{SW}_{ij} \qquad \forall ij \in \Omega_B, t \in \Omega_T, s \in \Omega_S \quad (14)$$

$$\left|P_{ij,t,s}\right| \le \overline{VI}_{ij} w^{SW}_{ij} \qquad \forall ij \in \Omega_B, t \in \Omega_T, s \in \Omega_S \quad (15)$$

$$\left|Q_{ij,t,s}\right| \le \overline{VI}_{ij} w^{SW}_{ij} \qquad \forall ij \in \Omega_B, t \in \Omega_T, s \in \Omega_S \quad (16)$$

$$\underline{V}^2 \le V^{SQ}_{i,t,s} \le \overline{V}^2 \qquad \forall i \in \Omega_N, t \in \Omega_T, s \in \Omega_S \quad (17)$$

$$(P^{SS}_{i,t,s})^2 + (Q^{SS}_{i,t,s})^2 \le \left(\overline{S}^{SS}_i\right)^2 \qquad \forall i \in \Omega_{SS}, t \in \Omega_T, s \in \Omega_S \quad (18)$$

In these constraints, the parameter $\overline{I}_{ij}$ is the current capacity of a branch and $\overline{S}^{SS}_i$ is the apparent power capacity of a SS. Constraint (14) is the current capacity limit for the branches, according to the statuses of their switches, (15) and (16) are the active and reactive power flows limits for the branches, also according with the statuses of the branches, (17) is the voltage limit for the nodes, and (18) is the apparent power capacity of the SSs.

### D. Model for the Operation of OLTCs and VRs

The operation of the OLTCs and VRs are modeled in (19)–(25) [21].

$$V^{SQ}_{j,t,s} = \sum_{k=0}^{2\overline{n}^{VR}_{ij}} \left\{ \left[1 + r^{VR}_{ij} \frac{(k - \overline{n}^{VR}_{ij})}{\overline{n}^{VR}_{ij}}\right]^2 V^C_{ij,k,t,s} \right\} \quad (19)$$

$$\theta_{i,t,s} = \theta_{j,t,s} \quad (20)$$

$$\forall ij \in \Omega_{VR}, t \in \Omega_T, s \in \Omega_S$$

$$\sum_{k=0}^{2\overline{n}^{VR}_{ij}} b^{VR}_{ij,k,t} = 1 \qquad \forall ij \in \Omega_{VR}, t \in \Omega_T \quad (21)$$

$$\underline{V}^2 b^{VR}_{ij,k,t} \le V^C_{ij,k,t,s} \le \overline{V}^2 b^{VR}_{ij,k,t} \quad (22)$$

$$\underline{V}^2 (1 - b^{VR}_{ij,k,t}) \le V^{SQ}_{i,t,s} - V^C_{ij,k,t,s} \le \overline{V}^2 (1 - b^{VR}_{ij,k,t}) \quad (23)$$

$$\forall ij \in \Omega_{VR}, k \in \{0, \cdots, 2\overline{n}^{VR}_{ij}\}, t \in \Omega_T, s \in \Omega_S$$

$$\sum_{t \in \Omega_T} (n^{VR+}_{ij,t} + n^{VR-}_{ij,t}) \le \delta^{VR}_{ij} \qquad \forall ij \in \Omega_{VR} \quad (24)$$

$$\sum_{k=0}^{2\overline{n}^{VR}_{ij}} [(k - \overline{n}^{VR}_{ij}) b^{VR}_{ij,k,t}] - \sum_{k=0}^{2\overline{n}^{VR}_{ij}} [(k - \overline{n}^{VR}_{ij}) b^{VR}_{ij,k,t-1}] = n^{VR+}_{ij,t} - n^{VR-}_{ij,t} \quad (25)$$

$$\forall ij \in \Omega_{VR}, t \in \Omega_T | t > 1$$

In these constraints, the parameters $\overline{n}^{VR}_{ij}$ is half of the number of tap positions of the VRs, $r^{VR}_{ij}$ is the maximum regulation of a VR, and $\delta^{VR}_{ij}$ is the maximum number of daily changes in the positions of a tap of a VR. The variables are: $V^C_{ij,k,t,s}$ is an auxiliary variable used to represent the nonlinear product $V^{SQ}_{i,t,s} b^{VR}_{ij,k,t}$, $b^{VR}_{ij,k,t}$ is a binary variable that indicates the tap position of a VR, and $n^{VR+}_{ij,t}$ and $n^{VR-}_{ij,t}$ are nonnegative auxiliary variables.

Constraint (19) calculates the value of the regulated voltage $V^{SQ}_{j,t,s}$ in terms of the auxiliary variable $V^C_{ij,k,t,s}$, which is calculated in (22) and (23). Constraint (20) defines the voltage angles at the terminal nodes of OLTCs and VRs, (21) requires that only one tap position can be selected in each time interval. Note that in (22) and (23), if $b^{VR}_{ij,k,} = 0$, then $V^C_{ij,k,t,s} = 0$. On the other hand, if $b^{VR}_{ij,k,} = 1$, then $V^C_{ij,k,t,s} = V^{SQ}_{i,t,s}$. Moreover, since only one tap position can be selected, (19) will calculate the regulated voltage in terms of the selected tap and the terminal voltage $V^{SQ}_{i,t,s}$. Finally, constraints (24) and (25) limit the number of changes in the position of the taps of each OLTC or VR during a day.

### E. Model for the Operation of CBs

The operation of the CBs is formulated using a voltage-dependent model, as presented in (26)–(31).

$$\hat{Q}^{CB}_{i,t,s} = \sum_{k=1}^{\overline{n}^{CB}_i} Q^{CB}_{i,k,t,s} \qquad \forall i \in \Omega_{CB}, t \in \Omega_T, s \in \Omega_S \quad (26)$$

$$-B^{CB}_i \overline{V}^2 (1 - b^{CB}_{i,k,t}) \le Q^{CB}_{i,k,t,s} - B^{CB}_i V^{SQ}_{i,t,s} \le -B^{CB}_i \underline{V}^2 (1 - b^{CB}_{i,k,t}) \quad (27)$$

$$B^{CB}_i \underline{V}^2 b^{CB}_{i,k,t} \le Q^{CB}_{i,k,t,s} \le B^{CB}_i \overline{V}^2 b^{CB}_{i,k,t} \quad (28)$$

$$\forall i \in \Omega_{CB}, k \in \{1, \cdots, \overline{n}^{CB}_{ij}\}, t \in \Omega_T, s \in \Omega_S$$

$$b^{CB}_{i,k,t} \le b^{CB}_{i,k-1,t} \qquad \forall i \in \Omega_{CB}, k \in \{2, \cdots, \overline{n}^{CB}_{ij}\}, t \in \Omega_T \quad (29)$$

$$\sum_{t \in \Omega_T} (n^{CB+}_{i,t} + n^{CB-}_{i,t}) \le \delta^{CB}_i \qquad \forall i \in \Omega_{CB} \quad (30)$$

$$\sum_{k=1}^{\overline{n}^{CB}_i} b^{CB}_{i,k,t} - \sum_{k=1}^{\overline{n}^{CB}_i} b^{CB}_{i,k,t-1} = n^{CB+}_{i,t} - n^{CB-}_{i,t} \quad (31)$$

$$\forall i \in \Omega_{CB}, t \in \Omega_T | t > 1$$

In these constraints, $\Omega_{CB}$ is the set of nodes with CBs. The parameter $\overline{n}^{CB}_i$ is the number of CBs module installed at a node, $B^{CB}_i$ is the susceptance of a CB module, and $\delta^{CB}_i$ is the maximum number of daily changes in the number of CB modules connected to a node. The variable $Q^{CB}_{i,k,t,s}$ is the reactive power injected by a BC module, $b^{CB}_{i,k,t}$ is a binary variable that indicates if a CB module is connected or not, and $n^{CB+}_{i,t}$ and $n^{CB-}_{i,t}$ are nonnegative auxiliary variables.

Constraint (26) provides the total reactive power injected by a CB at a node, (27) and (28) calculate the reactive power injected by each CB module. Note that, if $b^{CB}_{i,k,t} = 0$, then $Q^{CB}_{i,k,t,s} = 0$ in (28). On the other hand, if $b^{CB}_{i,k,t} = 1$, then $Q^{CB}_{i,k,t,s} = B^{CB}_i V^{SQ}_{i,t,s}$ in (27). Constraint (29) imposes a sequence for the connection of the CB modules, and is used to break symmetry in the model. Finally (30) and (31) are used to limit the number of changes in the number of modules of each CB connected to the system during a day.

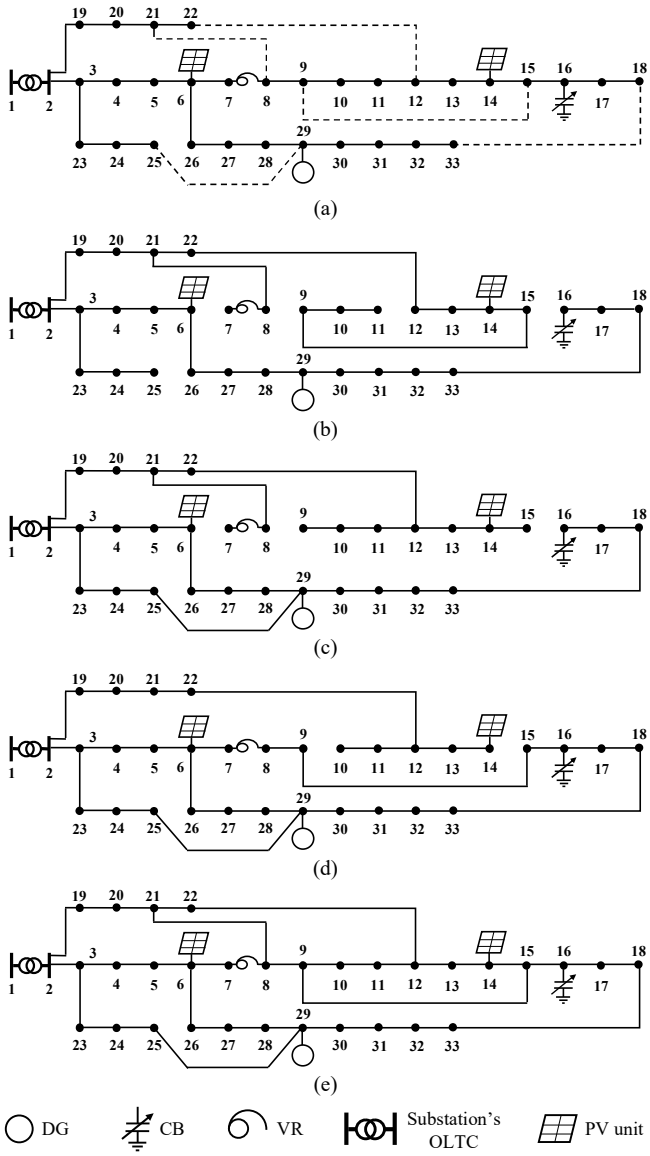


Figure 1. (a) Initial topology of the 33-node system, (b) radial solution for Case II, (c) closed-loop topology for Case III, (d) closed-loop topology for Case IV, and (e) topology with all branches closed for Case V.

### F. Model for Dispatchable DGs and PV Units

The capacities of the dispatchable DGs and PV units are considered in (32)–(36).

$$(P_{i,t}^{DG})^2 + (Q_{i,t}^{DG})^2 \leq \left(\overline{S}_i^{DG}\right)^2 \tag{32}$$

$$P_{i,t}^{DG} \geq 0 \tag{33}$$

$$-P_{i,t}^{DG}\tan(\cos^{-1}(\underline{\tau}_i)) \leq Q_{i,t}^{DG} \leq P_{i,t}^{DG}\tan(\cos^{-1}(\overline{\tau}_i)) \tag{34}$$
$$\forall i \in \Omega_{DG}, t \in \Omega_T$$

$$0 \leq P_{i,t,s}^{PV} \leq \lambda_{i,t,s}^{PV}\overline{P}_i^{PV} \tag{35}$$

$$-P_{i,t,s}^{PV}\tan(\cos^{-1}(\underline{\kappa}_i)) \leq Q_{i,t,s}^{PV} \leq P_{i,t,s}^{PV}\tan(\cos^{-1}(\overline{\kappa}_i)) \tag{36}$$
$$\forall i \in \Omega_{PV}, t \in \Omega_T, s \in \Omega_S$$

The parameter $\overline{S}_i^{DG}$ is the apparent power capacity of a DG, $\underline{\tau}_i$ and $\overline{\tau}_i$ are the power factor limits of the DGs, $\underline{\kappa}_i$ and $\overline{\kappa}_i$ are power factor limits of the PV units, $\lambda_{i,t,s}^{PV}$ is the generation factor of a PV generation unit, and $\overline{P}_i^{PV}$ is the rated capacity of a PV generation unit.

Constraint (32) is the apparent power generation capacity of the DGs, (33) requires that a DG can only inject active power into the system, (34) is the power factor limit for the DGs, (35) is the active power generation limit of a PV unit, and (36) is the power factor limit for the PV units.

TABLE I
COSTS OF THE RESULTS FOR THE 33-NODE SYSTEM (US$)

| Results | Case I | Case II | Case III | Case IV | Case V |
|---|---|---|---|---|---|
| Objective function | 8,634.74 | 8,308.74 | 8,233.27 | 8,205.61 | 8,217.98 |
| Losses | 265.10 | 199.59 | 187.03 | 191.43 | 177.80 |
| Operation of the SS | 5,941.03 | 5,752.09 | 5,704.26 | 5,681.87 | 5,697.17 |
| Operation of the DGs | 119.11 | 119.55 | 119.89 | 118.86 | 119.65 |
| Total carbon tax | 2,309.50 | 2,237.52 | 2,221.09 | 2,211.45 | 2,218.37 |
| Carbon tax of the SS | 2,271.98 | 2,199.86 | 2,183.32 | 2,174.01 | 2,180.68 |
| Carbon tax of the DG | 37.52 | 37.66 | 37.77 | 37.44 | 37.69 |

TABLE II
EXPECTED TOTAL $CO_2$ EMISSIONS (TONNES)

| Results | Case I | Case II | Case III | Case IV | Case V |
|---|---|---|---|---|---|
| DG | 227.20 | 219.95 | 218.30 | 217.35 | 218.03 |
| SS | 3.75 | 3.77 | 3.78 | 3.74 | 3.77 |
| Total | 230.95 | 223.72 | 222.08 | 221.09 | 221.80 |

### G. Topological Constraints

The connectivity of the system and the maximum number of loops allowed to be formed is controlled by (37)–(40).

$$|\Omega_N| - |\Omega_{SS}| \leq \sum_{ij\in\Omega_B} w_{ij}^{SW} + |\Omega_{VR}| \leq |\Omega_N| - |\Omega_{SS}| + N^{LP} \tag{37}$$

$$\sum_{ji\in\Omega_B} f_{ji} - \sum_{ij\in\Omega_B} f_{ij} + \sum_{ji\in\Omega_{VR}} f_{ji}^{VR} - \sum_{ij\in\Omega_{VR}} f_{ij}^{VR} + g_i = 1 \tag{38}$$
$$\forall i \in \Omega_N$$

$$|f_{ij}| \leq |\Omega_N| w_{ij}^{SW} \qquad \forall ij \in \Omega_B \tag{39}$$

$$0 \leq g_i \leq |\Omega_N| \qquad \forall i \in \Omega_{SS} \tag{40}$$

The parameter $N^{LP}$ is the maximum number of basic loops allowed to be formed in the system. The variables $f_{ij}$ and $f_{ij}^{VR}$ are artificial flows on branches and VRs, respectively, and $g_i$ is an artificial generation at SS nodes. Constraint (37) is used to control the number of loops in the system together with (38)–(40), that ensure the connectivity of the system, i.e., that there must be a path from each node of the system to a SS.

## III. TESTS AND RESULTS

A 33-node system, available in [22] and shown in Fig. 1 (a), is used to test the proposed model. This system operates at a nominal voltage of 12.66 kV. The existent generation of the system is composed of one 250 kVA dispatchable DG at node 29 with power factor limits $\underline{\tau}_i = \overline{\tau}_i = 0.80$, and two PV generation units at nodes 6 and 14, each one with a capacity of 250 kW and power factor limits $\underline{\kappa}_i = \overline{\kappa}_i = 0.90$. A switchable CB with four modules of 150 kVAr each is installed at node 16. A VR is installed at branch 7–8 with a regulation capacity of ±10% and ±8 positions. Finally, the SS is equipped with an OLTC with a regulation capacity of ±5% and ±2 steps. The grid and dispatchable DG emission intensities are 2.17 kg $CO_2$/kWh and 0.63 kg $CO_2$/kWh, respectively. The data used to determine the behavior of the system are obtained from [23], and the *k*-means clustering technique [24] is used to reduce it to a suitable set of stochastic scenarios, as explained in [25]. In this way, the behavior of load, solar irradiation, and energy prices are represented by 24 scenarios, divided into twelve time intervals with two scenarios each.

The optimization model was implemented in AMPL [26] and solved with the solver CPLEX 12.10.0 [27] with an optimality gap of 0.10%. Numerical experiments were processed on a computer with a 3.20 GHz Intel® Core™ i7-8700 processor and 32 GB of RAM.


Figure 2. (a) Active power injected by the dispatchable DG at node 29, (b) reactive power injected by the dispatchable DG at node 29, (c) active power injected by the PV unit at node 6, (d) reactive power injected by the PV unit at node 6, (e) active power injected by the PV unit at node 14, (f) reactive power injected by the PV unit at node 14, (g) tap positions of the SS's OLTC, (h) tap positions of the VR, (i) operation of the CB at node 16.

Five cases are analyzed, in all of them the VR's and OLTC's tap positions, the CB operation, and the dispatch of the generation units are optimized. In Case I, network reconfiguration is not allowed. In Case II, network reconfiguration is considered, however, the network topology is required to be radial. Case III considers network reconfiguration allowing the formation of a single loop. Case IV considers network reconfiguration allowing the formation of up to five basic loops, i.e., the model will find the optimal number of basic loops that optimize the operation of the system. Finally, Case V considers all branches operating connected to the system.

For all the cases, Fig. 1 (a)–(e), shows the optimal topologies of the system, while Fig. 2 presents the results related to the operation of the system for Cases I–V. Table I presents the operational costs of the system for all cases. Table II shows the expected values of $CO_2$ emissions.

The complete operations of the dispatchable DGs, PV units, and voltage control devices are presented in Fig. 2 for Cases I–V. In Fig. 2 (a), the active power injection of the dispatchable DG at node 29 stays almost constant throughout the day. Fig. 2 (b) shows the variations of the reactive power injected by the dispatchable DG at node 29 for all cases. The

active and reactive power injections by the PV units at nodes 6 and 14 are presented in Fig. 2 (c)–(f), and, as expected, the active power injections follow the solar irradiation of the stochastic scenarios. For both PV units, the active power injected have similar behaviors, however, the reactive power injected have different profiles. Fig. 2 (g) and (h) show the operation of the OLTC and the VR at branch 6–8. The operation of the CB at node 16 is presented in Fig. 2 (i).

The results presented in Table I indicate that, in Cases III, IV, and V, the reconfiguration considering closed-loop operation improves the objective function. Taking Case I as a reference, the network reconfiguration with closed-loop operation allows improving the objective function in 4.65% in Case III, 4.97% in Case IV, and 4.83% in Case V. Moreover, by comparing the results of Cases II, in which a radial topology of the system is required for the reconfiguration problem, and Cases IV and V, reductions of 1.24% and 1.09% are obtained, respectively. The tests indicate that three or more basic loops do not improve the objective function of the problem beyond the value obtained for Case IV. Note that, when all branches of the system are in operation (Case V), the value of the objective function is 0.15% greater than the value of the solution for Case IV. The major impact in the objective function is in the reduction of the operational cost related to the energy purchased from the SS and in the losses cost, which also leads to a reduction of the total $CO_2$ emissions in the system. In this regard, the network reconfiguration reduces the $CO_2$ emissions in 7.23, 8.87, 9.86, and 9.15 tonnes for Cases II, III, IV, and V, respectively, when compared to Case I.

A final test was conducted considering only the possibility of closing the open branches, maintaining the initial closed branches connected to the system. In this case, the solution is the same as the one obtained for Case V. This highlights the importance of considering network reconfiguration together with loops formation in the problem.

## IV. Conclusion

This paper presented a new stochastic mixed-integer second-order cone programming model for the problem of optimal operation of active distribution systems considering network reconfiguration, voltage control devices, dispatchable and nondispatchable distributed generators, and the possibility of closed-loop operation. The obtained results showed lower operational costs, reduced losses, and greenhouse gas emissions mitigation when reconfiguration with closed-loop topologies was considered. Moreover, it was demonstrated that the solution with all branches in operation may not be the best solution for the problem. Thus, the alternative of allowing closed-loop topologies in active distribution systems can provide more efficient and environmentally-friendly network operation schemes.

## References


[1] G. W. Stagg and A. H. El-Abiad, *Computer methods in power system analysis*, 1st ed. New York: McGraw-Hill, 1968.

[2] A. Augugliaro, L. Dusonchet, S. Favuzza, and E. R. Sanseverino, "Voltage regulation and power losses minimization in automated distribution networks by an evolutionary multiobjective approach," *IEEE Trans. Power Syst.*, vol. 19, no. 3, pp. 1516–1527, Aug. 2004.

[3] Y. P. Agalgaonkar, B. C. Pal, and R. A. Jabr, "Distribution voltage control considering the impact of PV generation on tap changers and autonomous regulators," *IEEE Trans. Power Syst.*, vol. 29, no. 1, pp. 182–192, Jan. 2014.

[4] R. A. Araujo, P. C. M. Meira, and M. C. de Almeida, "Algorithms for operation planning of electric distribution networks," *J. Control. Autom. Electr. Syst.*, vol. 24, no. 3, pp. 377–387, Jun. 2013.

[5] A. Padilha-Feltrin, D. A. Quijano Rodezno, and J. R. S. Mantovani, "Volt-VAr multiobjective optimization to peak-load relief and energy efficiency in distribution networks," *IEEE Trans. Power Deliv.*, vol. 30, no. 2, pp. 618–626, Apr. 2015.

[6] M. A. M. Shaheen, H. M. Hasanien, S. F. Mekhamer, and H. E. A. Talaat, "Optimal power flow of power systems including distributed generation units using sunflower optimization algorithm," *IEEE Access*, vol. 7, pp. 109289–109300, 2019.

[7] V. B. Pamshetti, S. Singh, and S. P. Singh, "Combined impact of network reconfiguration and volt-VAr control devices on energy savings in the presence of distributed generation," *IEEE Syst. J.*, vol. 14, no. 1, pp. 995–1006, Mar. 2020.

[8] J. Wang, W. Wang, Z. Yuan, H. Wang, and J. Wu, "A chaos disturbed beetle antennae search algorithm for a multiobjective distribution network reconfiguration considering the variation of load and dg," *IEEE Access*, vol. 8, pp. 97392–97407, 2020.

[9] T. Fetouh and A. M. Elsayed, "Optimal control and operation of fully automated distribution networks using improved tunicate swarm intelligent algorithm," *IEEE Access*, vol. 8, pp. 129689–129708, 2020.

[10] J. Martínez-Crespo and H. M. Khodr, "Integral methodology for distribution systems reconfiguration based on optimal power flow using Benders decomposition technique," *IET Gener. Transm. Distrib.*, vol. 3, no. 6, pp. 521–534, Jun. 2009.

[11] R. A. Jabr, "Minimum loss operation of distribution networks with photovoltaic generation," *IET Renew. Power Gener.*, vol. 8, no. 1, pp. 33–44, Jan. 2014.

[12] R. R. Gonçalves, R. P. Alves, J. F. Franco, and M. J. Rider, "Operation planning of electrical distribution systems using a mixed integer linear model," *J. Control. Autom. Electr. Syst.*, vol. 24, no. 5, pp. 668–679, Oct. 2013.

[13] S. Paudyal, C. A. Canizares, and K. Bhattacharya, "Optimal operation of distribution feeders in smart grids," *IEEE Trans. Ind. Electron.*, vol. 58, no. 10, pp. 4495–4503, Oct. 2011.

[14] Y. Liu, J. Li, and L. Wu, "Coordinated optimal network reconfiguration and voltage regulator/DER control for unbalanced distribution systems," *IEEE Trans. Smart Grid*, vol. 10, no. 3, pp. 2912–2922, May 2019.

[15] L. Gutierrez-Lagos and L. F. Ochoa, "OPF-based CVR operation in PV-rich MV–LV distribution networks," *IEEE Trans. Power Syst.*, vol. 34, no. 4, pp. 2778–2789, Jul. 2019.

[16] Y. Liu, L. Guo, C. Lu, Y. Chai, S. Gao, and B. Xu, "A fully distributed voltage optimization method for distribution networks considering integer constraints of step voltage regulators," *IEEE Access*, vol. 7, pp. 60055–60066, 2019.

[17] G. C. Kryonidis, C. S. Demoulias, and G. K. Papagiannis, "A two-stage solution to the bi-objective optimal voltage regulation problem," *IEEE Trans. Sustain. Energy*, vol. 11, no. 2, pp. 928–937, Apr. 2020.

[18] T.-H. Chen, W.-T. Huang, J.-C. Gu, G.-C. Pu, Y.-F. Hsu, and T.-Y. Guo, "Feasibility study of upgrading primary feeders from radial and open-loop to normally closed-loop arrangement," *IEEE Trans. Power Syst.*, vol. 19, no. 3, pp. 1308–1316, Aug. 2004.

[19] D. Ritter, J. F. Franco, and R. Romero, "Analysis of the radial operation of distribution systems considering operation with minimal losses," *Int. J. Electr. Power Energy Syst.*, vol. 67, pp. 453–461, May 2015.

[20] L. M. Hajagos and B. Danai, "Laboratory measurements and models of modern loads and their effect on voltage stability studies," *IEEE Trans. Power Syst.*, vol. 13, no. 2, pp. 584–592, May 1998.

[21] L. H. Macedo, J. F. Franco, M. J. Rider, and R. Romero, "Optimal operation of distribution networks considering energy storage devices," *IEEE Trans. Smart Grid*, vol. 6, no. 6, pp. 2825–2836, Nov. 2015.

[22] "LaPSEE power system test cases repository," 2021. [Online]. Available: http://www.feis.unesp.br/#!/lapsee. [Accessed: 01-Feb-2021].

[23] S. Pfenninger and I. Staffell, "Renewables.ninja," 2020. [Online]. Available: https://www.renewables.ninja/. [Accessed: 01-Nov-2020].

[24] J. Wu, *Advances in k-means clustering: a data mining thinking*, 1st ed. Berlin, Germany: Springer-Verlag, 2012.

[25] J. M. Home-Ortiz, M. Pourakbari-Kasmaei, M. Lehtonen, and J. R. Sanches Mantovani, "Optimal location-allocation of storage devices and renewable-based DG in distribution systems," *Electr. Power Syst. Res.*, vol. 172, pp. 11–21, Jul. 2019.

[26] R. Fourer, D. M. Gay, and B. W. Kernighan, *AMPL: a modeling language for mathematical programming*, 2nd ed. Duxbury, MA, USA: Thomson, 2003.

[27] IBM, "IBM ILOG CPLEX optimization studio v12.10.0 documentation," 2020. [Online]. Available: https://www.ibm.com/support/knowledgecenter/en/SSSA5P_12.10.0/COS_KC_home.html. [Accessed: 14-Sep-2020].